

# A new Extended Main Sequence Turnoff star cluster in the Large Magellanic Cloud

Andrés E. Piatti\*

*Instituto de Astronomía y Física del Espacio, CC 67, Suc. 28, 1428, Ciudad de Buenos Aires, Argentina*

8 January 2013

## ABSTRACT

We present results on the age and metallicity estimates of the poorly studied LMC cluster SL 529, from CCD SDSS *gr* photometry obtained at the Gemini South telescope with the GMOS attached. The cluster MSTO region possesses an extended structure, with an age spread ( $\sim 0.5$  Gyr) bigger than the mean age width of known EMSTO LMC clusters. We report for the first time a mean cluster age of 2.25 Gyr and a mean cluster metallicity of  $Z=0.004$ , which place it as the most metal-poor and oldest cluster in the EMSTO LMC cluster group. In addition, the cluster RC appears to be formed by two concentrations of stars - although it is not clear whether this feature can be caused, in part, by binary interactions and mergers -, whereas the cluster core radius of 4.2 pc is in excellent agreement with those determined for the previously 12 known EMSTO LMC clusters.

**Key words:** techniques: photometric – galaxies: individual: LMC – Magellanic Clouds – galaxies: star clusters.

## 1 INTRODUCTION

Up to date, only 12 Large Magellanic Cloud (LMC) star clusters have been uncovered to possess Extended Main Sequence Turnoffs (EMSTOs), namely: NGC 1751, 1783, 1806, 1846, 1852, 1917, 1987, 2108, 2154, 2173, Hodge 7, and SL 862 (see, e.g., Bertelli et al. 2003, Milone et al. 2009). The age range of this cluster sample is  $\sim 1$ -2 Gyr, while a roughly constant metal content of  $[\text{Fe}/\text{H}] = -0.4$  dex has been reported for them Mackey & Broby Nielsen (2007), Mackey et al. (2008), Goudfrooij et al. (2009), Girardi et al. (2009). These age and metallicity ranges coincide with those of an important bursting cluster formation epoch that took place in the LMC  $\sim 2$  Gyr ago, possible due the tidal interaction between both Magellanic Clouds and, perhaps, also the Milky Way. Particularly, Piatti (2011) found that the number of studied clusters with ages between 1 and 3 Gyr now doubles that of the population of clusters formed at the bursting epoch, thus increasing the probability that more EMSTO star clusters be identified. However, from a total of some 70 star clusters with age estimates within our age range of interest, the list of known EMSTO clusters has remained unchanged. The relatively small number of known EMSTO LMC star clusters is even more noticeable when considering the 2268 star clusters cataloged in the LMC (Bonatto &

Bica, 2010), thus representing  $\sim 3\%$  of the estimated LMC population of clusters formed at the bursting epoch.

In this paper, we report for the first time age and metallicity estimates for SL 529 (R.A. =  $5^{\text{h}}31^{\text{m}}06^{\text{s}}$ , Dec. =  $-63^{\circ}32'23''$ , J2000), a poorly studied LMC star cluster located in the outer disk of the galaxy. The results show that this cluster belongs to the handful of EMSTO clusters in the LMC. The impact of this finding would appear to be twofold: first, we actually found a new LMC cluster formed at the beginning of the bursting formation epoch which exhibits the EMSTO phenomenon. To this respect, we do show not only evidence about the age spread in the cluster MSTO, but also that the magnitude of the age spread exhibited by its stellar populations is correlated with the cluster core radius (Keller et al. 2011). Additionally, we identified two concentrations of stars in Red Clump (RC), although it is not clear whether this feature can be caused, in part, by binary interactions and mergers (Yang et al. 2011).

Second, SL 529 resulted to be the oldest (age  $\sim 2.25$  Gyr) and the most metal-poor EMSTO LMC cluster ( $[\text{Fe}/\text{H}] \sim -0.7$  dex). The cluster age is close to the limit estimated by Keller et al. (2011, age  $\sim 2.3$  Gyr) from which the age spread of the cluster stellar populations represents a diminishing fraction of the cluster age, so that the multiple populations become increasingly harder to resolve photometrically. On the other hand, the resulting cluster metallicity is lower than any known 1-3 Gyr old LMC cluster (Piatti & Geisler 2012),

\* E-mail: andres@iafe.uba.ar

making it an interesting case to constrain EMSTO models at different overall chemical abundance levels.

This paper is organized as follows. In Section 2 we describe the data collected, the reduction procedures performed, and the subsequent photometry standardization. Section 3 deals with the analysis of the data, from which cluster age, metallicity, reddening and structural parameters have been derived. In this Section we provide with observational evidence about the status of SL 529 as an EMSTO LMC cluster. Finally, we summarize our results in Section 4.

## 2 DATA HANDLING

Based on data obtained from the Gemini Science Archive, we collected CCD SDSS  $gr$  (Fukugita et al., 1996) images centred on 26 LMC clusters (GS-2010B-Q-74, PI: Pessev) along with observations of standard fields and calibration frames (zero, sky-flat, dome-flat). The data were obtained at the Gemini South telescope with the Gemini Multi-Object Spectrograph (GMOS) attached (scale =  $0.146 \text{ pixel}^{-1}$ ). The data consist in 2 exposures of 30 s in  $g$  and 2 exposures of 15 s in  $r$  for each cluster under seeing conditions better than  $0''.6$  and with airmass of 1.25-1.40. Nine Gemini Observatory standard fields were observed along the 5 cluster observing nights, for which 2 exposures of 5 s per filter and airmass in the range  $\sim 1.0$ -2.0 were obtained.

The data reduction followed the procedures documented by the Gemini Observatory webpage<sup>1</sup> and the IRAF<sup>2</sup>.GMOS package. We processed a total of 118 images (standard star and cluster fields) by performing overscan, trimming corrections, bias subtraction, flattened all data images, etc., once the calibration frames (zeros, sky- and dome-flats, etc.) were properly combined. The final field of view of the images resulted to be  $\sim 5'.6 \times 5'.6$ .

Depending on the night, nearly 30-50 independent magnitude measures of standard stars were derived per filter using the APPHOT task within IRAF, in order to secure the transformation from the instrumental to the SDSS  $gr$  standard system. The relationships between instrumental and standard magnitudes were obtained by fitting the following equations:

$$g = g_1 + g_{std} + 0.18 \times X_g + g_2 \times (g - r)_{std} \quad (1)$$

$$r = r_1 + r_{std} + 0.10 \times X_r + r_2 \times (g - r)_{std} \quad (2)$$

where  $g_i$ , and  $r_i$  ( $i=1,2$ ) are the fitted coefficients, and  $X$  represents the effective airmass. We solved the transformation equations with the FITPARAMS task in IRAF and found mean colour terms of  $-0.058$  in  $g$ ,  $-0.049$  in  $r$ . The rms errors from the transformation to the standard system were  $0.015 \text{ mag}$  for  $g$  and  $0.023$  for  $r$ , respectively, indicating an excellent photometric quality.

The stellar photometry was performed using the starfinding and point-spread-function (PSF) fitting routines

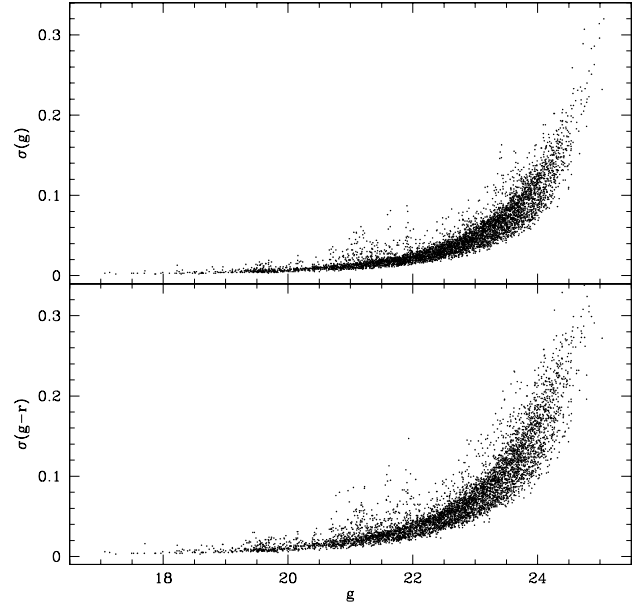


**Figure 1.** Magnitude and colour errors as a function of  $g$  for stars which passed all the required photometric restrictions.

in the DAOPHOT/ALLSTAR suite of programs (Stetson et al. 1990). For each image, a quadratically varying PSF was derived by fitting  $\sim 60$  stars, once the neighbours were eliminated using a preliminary PSF derived from the brightest, least contaminated  $\sim 20$  stars. Both groups of PSF stars were interactively selected. We then used the ALLSTAR program to apply the resulting PSF to the identified stellar objects and to create a subtracted image which was used to find and measure magnitudes of additional fainter stars. This procedure was repeated three times for each frame. After deriving the photometry for all detected objects in each filter, a cut was made on the basis of the parameters returned by DAOPHOT. Only objects with  $\chi < 2$ , photometric error less than  $2\sigma$  above the mean error at a given magnitude, and  $|\text{SHARP}| < 0.5$  were kept in each filter.

Finally, we standardized the resulting instrumental magnitudes and combined all the independent measurements using the stand-alone DAOMATCH and DAOMASTER programs, which were kindly provided by Peter Stetson. The final information consists of a running number per star, its  $x$  and  $y$  coordinates, the mean  $g$  magnitudes and  $g - r$  colours, the standard errors  $\sigma(g)$  and  $\sigma(g - r)$ , and the number  $n$  of averaged magnitudes and colours. A portion of Table 1, which gives this information for a total of 5454 stars in the field of SL 529, is shown here for guidance regarding its form and content, while Fig. 1 shows the obtained magnitude and colour errors. The whole content of Table 1 is available in the online version of the journal. The photometric information gathered for the remaining 25 clusters will be presented in a forthcoming paper.

## 3 DATA ANALYSIS

The cluster centre  $[(x_c, y_c) = (1520 \pm 10, 1100 \pm 10) \text{ pixels}]$  was estimated using the NGAUSSFIT task within the

<sup>1</sup> <http://www.gemini.edu/sciops/instruments/?q=sciops/instruments>

<sup>2</sup> IRAF is distributed by the National Optical Astronomy Observatories, which is operated by the Association of Universities for Research in Astronomy, Inc., under contract with the National Science Foundation.

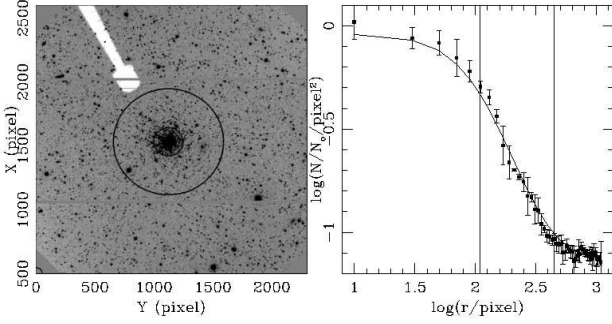


**Figure 2.** *Left panel:* 15 s exposure  $r$  image centred on SL 529. The circles corresponding to  $r_c$  and  $r_{cls}$  are also drawn. *Right panel:* The cluster stellar radial profile (filled box) with the derived errorbars, and the best-fitted King (1962) model superimposed. The vertical lines represent  $r_c$  and  $r_{cls}$ .

IRAF.STSDAS package. We then constructed the cluster radial profile depicted in Fig. 2 (right panel), which served us to adopt the cluster radius ( $r_{cls}$ ) - defined as the distance from the cluster centre where the stellar density profile intersects the background level- to perform circular extractions in the Colour-Magnitude Diagram (CMD). We also fitted a King (1962) model to the normalized radial stellar density profile using the expression:

$$N/N_o = \left( \frac{1}{\sqrt{1 + (r/r_c)^2}} - \frac{1}{\sqrt{1 + (r_t/r_c)^2}} \right)^2 + bkg \quad (3)$$

where  $N_o$  is the central stellar density, and  $r_c$  and  $r_t$  are the core and tidal radii, respectively.  $bkg$  represents the background level. The values for  $r_c$ ,  $r_{cls}$ , and  $r_t$  turned out to be  $(110 \pm 10)$  pixels,  $(450 \pm 50)$  pixels, and  $(1300 \pm 100)$  pixels, respectively. Circles centred on the cluster with radii  $r_c$  and  $r_{cls}$  are drawn in the left panel of Fig. 2, and they are also indicated with vertical lines in the right panel of the figure.

We built two CMDs centred on the cluster, one for a circular extraction of radius  $r_{cls}$ , and another with an inner radius  $2 \times r_{cls}$  and equal area as for the cluster. The resulting cluster and field CMDs are shown in Fig. 3. As can be seen, the cluster MSTO appears noticeably extended, the cluster RC shows a dual structure, and the cluster Red Giant Branch (RGB) resembles that of a single overall metallicity. All these features suggest that SL 529 could be included from now on in the list of known EMSTO LMC clusters.

In order to estimate the mean cluster age, we adopted a distance modulus of  $(m - M)_o = 18.50 \pm 0.10$  (Glatt et al. 2010). The reddening value was taken from the Burstein & Heiles (1982), and Schlegel, Finkbeiner, & Davis (1998) extinction maps, adopting a weighted average value of  $E(B - V) = 0.04 \pm 0.01$ , since both the small reddening values as well as their errors suggest that no differential reddening would affect the cluster. We adopted  $R = A_V/E(B - V) = 3.1$  to convert the colour excess to the extinction, and used the equations  $A_g/A_V = 1.199$  and  $A_r/A_V = 0.858$  (Fan 1999) to evaluate the total extinctions in  $A_g$  and  $A_r$ . Finally, we used  $E(g - r)/A_V = 0.341$  for the selective extinction in the SDSS system.

When we chose subsets of isochrones for different  $Z$  metallicity values to evaluate the metallicity effect in the cluster age, we preferred to follow the general rule of start-

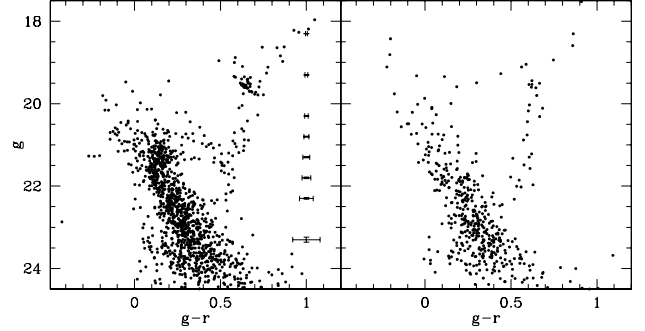


**Figure 3.** Colour-Magnitude diagrams of SL 529 (left) and of its surrounding field (right) for an equal cluster area. The magnitude and colour errorbars are also indicated.

ing without assuming any prearranged metallicity. Instead, we adopted chemical compositions of  $Z = 0.002$ ,  $0.004$  and  $0.008$  ( $[\text{Fe}/\text{H}] = -1.0, -0.7, \text{ and } -0.4$ , respectively) for the isochrone sets which cover the metallicity range of most of the intermediate-age LMC clusters studied in detail so far (Piatti & Geisler 2012). We then selected a set of isochrones of Marigo et al. (2008) and superimposed them on the cluster CMD, once they were properly shifted by the corresponding  $E(B - V)$  colour excesses and by the adopted LMC apparent distance modulus. Finally, we adopted as the cluster age the one corresponding to the isochrone of age = 2.25 Gyr and  $Z = 0.004$  which best reproduces the cluster main features in the CMD. Fig. 4 shows the result of the fitting, wherein we plotted the isochrone of the adopted cluster age and two additional isochrones bracketing the derived age. The bracketing isochrones (age = 2.0 and 2.5 Gyr) were fitted by taking into account the observed spread in the cluster MSTO. We would like to note that the estimated cluster age and metallicity place it as the most metal-poor and oldest EMSTO LMC cluster.

In order to quantify the MSTO extension we counted the number of stars ( $N$ ) located within the rectangle drawn in Fig. 5, using as independent variable the coordinate ( $X$ ) along the long axis, according to the precepts outlined by Goudfrooij et al. (2011, see their Fig. 14). The resulting field subtracted histogram is depicted in Fig. 6, which clearly exhibits an extended distribution. When building the histogram we have taken into account the effects caused by using different binning as well as the point errors, which cause the points have the chance to fall outside their own bin if they do not fall in the bin centre (Piatti & Geisler 2012); thus producing an intrinsic distribution. Fig. 6 also compares this resulting distribution with those of Goudfrooij et al. (2011) for the known EMSTO LMC clusters NGC 1751 (blue line), NGC 1783 (red line), NGC 1806 (yellow line), NGC 1987 (magenta line), and NGC 2108 (cyan line), previously normalized to the unity and shifted in order to superimpose the youngest ends. As can be seen, the most important result is that we confirm the existence of an EMSTO ( $\sim 0.5$  Gyr) for SL 529, which is bigger than the mean age width of known EMSTO clusters (Milone et al. 2009; Goudfrooij et al. 2011).

The magnitude of the age spread exhibited by the stellar population of an EMSTO cluster is correlated with the cluster core radius (Keller et al. 2011). The 12 known EM-

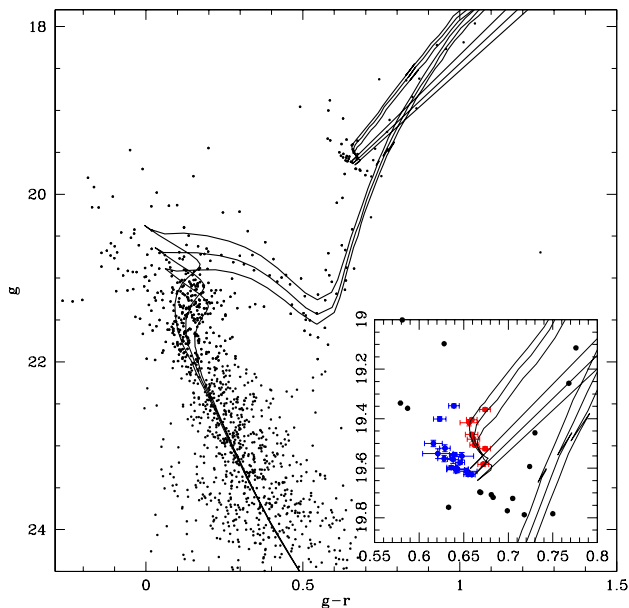


**Figure 4.**  $g$  versus  $g - r$  cluster CMD with isochrones of Marigo et al. (2008) for  $t = 2.0, 2.25,$  and  $2.5$  Gyr and  $Z = 0.004$  superimposed. The inner panel depicts an enlargement of the RC region, wherein two groups of RC stars have been represented with blue and red circles.

STO clusters do have core radii bigger than  $r_c \sim 3.7$  pc. In the case of SL 529, we used the derived cluster core radius (in pixels) and the recently estimated LMC distance of  $(53.5 \pm 0.4)$  kpc (Haschke et al. 2012) to obtain  $r_c = (4.20 \pm 0.35)$  pc. When entering this core radius and the cluster age in their Fig. 5, SL 529 falls into the visibility window of EMSTO clusters, for which different authors have argued that they are witnesses of different/prolonged stellar formation epochs (Keller et al., 2012, and references therein).

Indeed, Mackey et al. (2008) built synthetic CMDs to investigate the role played by unresolved binary stars around the MSTO region of three LMC clusters (NGC 1783, 1806, and 1846). They found that the resulting CMDs for a single population -corresponding to an isochrone with the age and metallicity of the respective cluster- do not reproduce alone the EMSTOs seen in the studied clusters, although they included a significant fraction of unresolved binaries. However, when considering two stellar populations, beside a fraction of unresolved binaries, the resulting CMDs reproduce better the observed ones. The age spread of these three clusters turned out to be  $\sim 0.3$ - $0.4$  Gyr. Similarly, Goudfrooij et al. (2011) argued that the impact of interacting binaries as suggested by Yang et al. (2011) in the CMDs of 7 EMSTOs LMC clusters studied by them ( $\Delta(\text{age}_{MSTO}) = 0.35 \pm 0.10$  Gyr) is insignificant. They concluded that the placement in their CMDs of these binaries stars most likely correspond to that of LMC field stars. They are a low stellar density population in the CMD towards brighter magnitudes and bluer colours than the cluster MSTO. Milone et al. (2009), among others, also claimed that taking into account the presence of binary stars alone in intermediate-age LMC clusters is not enough to reproduce their observed EMSTOs ( $\Delta(\text{age}) \gtrsim 0.3$  Gyr). According to these results and bearing in mind the age

spread found for the SL 529's MSTO, we also infer that more than one stellar population would appear to be required to explain the morphology of the MSTO region. Recently, Li et al. (2012) have shown that most CMDs, including extended or multiple TOs, can be explained using simple stellar populations including both binary and stellar rotation effects, or composite populations with two components.

Dual red clumps (RCs) have also been observed in some star clusters with or without EMSTOs (Girardi et al. 2010). However, while Girardi et al. (2009) suggested that the origin for such a structure is related to an age spread, Yang et al. (2011) found that part of the observed dual RCs may be the result of binary interactions and mergers. In order to highlight the RC structure of SL 529 we plotted in Fig. 4 an enlargement of the RC region, where two groups of stars have been represented with blue and red circles. The error-bar represents the star photometric errors. Notice that all the stars are located within  $r_{cls}$  (see Fig. 1), and a slightly more populated picture would be obtained if we included cluster red giants spread within  $1.5r_{cls}$ . The additional RC stars would have reached the outer cluster region due to the dynamical relaxation (Santiago 2009). Particularly, some four stars would be added around  $(g - r, g) \sim (0.6, 19.8)$  mag. We think that this handful of stars does not constitute a clear evidence of the existence of a secondary RC as suggested by Girardi et al. (2009). On the other hand, the RC interacting binaries modeled by Yang et al. (2011, see red points in their Fig. 1) would appear to cover the RC region as well as to reach fainter magnitudes ( $\Delta V < 0.5$  mag) and bluer colours ( $\Delta(V - I) < 0.1$  mag). Unfortunately, they did not present CMDs for ages larger than 1.8 Gyr, although they mentioned that interacting binaries appear mainly in clusters with  $1.2 \text{ Gyr} < \text{age} < 3.0 \text{ Gyr}$ . Despite the lack of a direct transformation of our  $(g - r, g)$  CMD to their  $(V - I, V)$  one, the overall appearance of both RCs would seem to be similar. Further spectroscopic studies are still needed in order to obtain more reliable membership status and to confirm whether the cluster RC actually contains a binary star population. We would like to point out, however, that the age sequence in the single stellar population models of Yang et al. runs perpendicular to that of the Marigo et al.'s isochrones.

## 4 SUMMARY

In this study we present for the first time CCD SDSS  $gr$  photometry of stars in the field of the poorly studied LMC cluster SL 529. The data were obtained at the Gemini South telescope with the GMOS attached under high quality photometric conditions. We are confident that the photometric data yield accurate morphology and position of the main cluster features in the CMD. The analysis of the cluster MSTO region shows that SL 529 possesses an extended MSTO of  $\sim 0.5$  Gyr. We thus report that SL 529 belongs to the group of the EMSTO LMC clusters. We estimated the cluster age and metallicity by fitting theoretical isochrones to its CMD, previously shifted by its  $E(B - V)$  colour excess and apparent distance modulus. The isochrone which best reproduces the cluster features turns out to be that of 2.25 Gyr and  $Z=0.004$ , with an observed age spread of  $\pm 0.25$

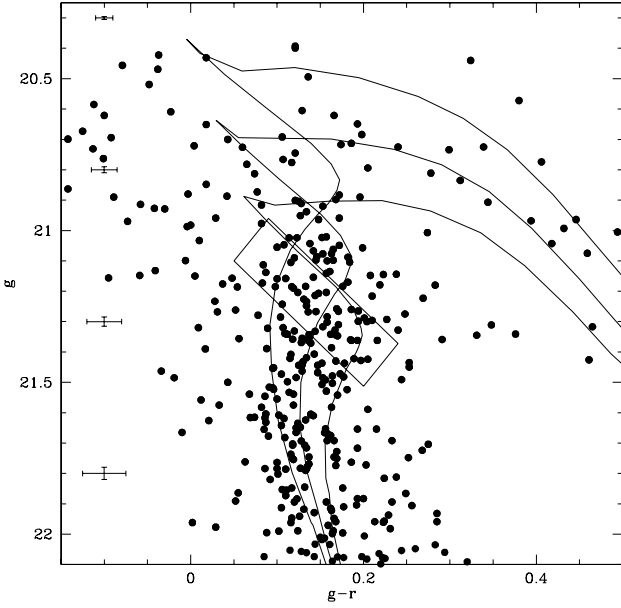


**Figure 5.** Enlargement of the CMD of SL 529, focusing on the EMSTO region, with isochrones of Marigo et al. (2008) for ages of 2.0, 2.25, and 2.5 Gyr, overplotted. A rectangle scanning the MSTO region is also superimposed.

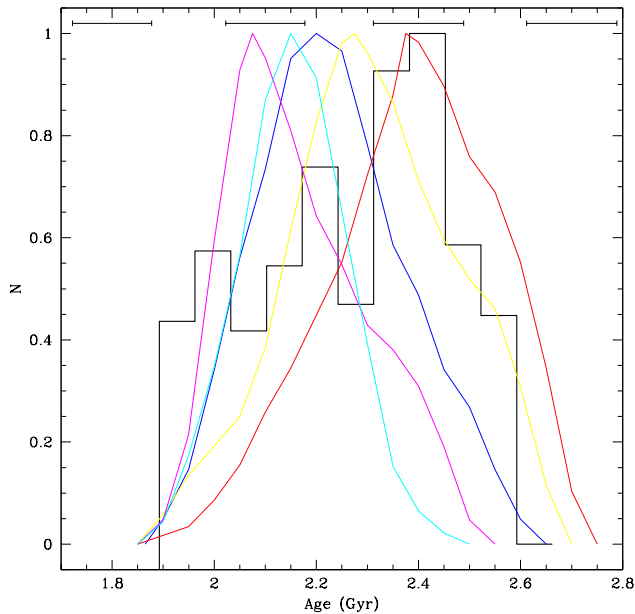


**Figure 6.** Number of stars counted along the major axis of the rectangle drawn in Fig. 5. The normalized MSTO distributions for NGC 1751 (blue line), NGC 1783 (red line), NGC 1806 (yellow line), NGC 1987 (magenta line), and NGC 2108 (cyan line) from Goudfrooij et al. (2011), are overplotted. The age errorbars spanning  $2\sigma$  are also illustrated.

Gyr. The estimated cluster age and metallicity place it as the most metal-poor and oldest EMSTO LMC cluster.

In addition, we also found that the cluster RC appears to be formed by two concentrations of stars, although it is not clear whether this feature can be caused, in part, by binary interactions and mergers. Finally, we fitted a King profile to the cluster stellar density radial distribution and obtained a core radius of  $(4.20 \pm 0.35)$  pc, if a LMC distance of  $(53.5 \pm 0.4)$  kpc is adopted. This value reinforces the status of SL 529 as a EMSTO cluster, since it is in excellent agreement with those determined for the 12 known EMSTO LMC clusters.

#### ACKNOWLEDGEMENTS

We greatly appreciate the comments and suggestions raised by the reviewer which helped me to improve the manuscript. This work was partially supported by the Argentinian institutions CONICET and Agencia Nacional de Promoción Científica y Tecnológica (ANPCyT).

#### REFERENCES

- Bertelli G., Nasi E., Girardi L., et al. 2003, *AJ*, 125, 770  
 Bonatto C., Bica E. 2010, *MNRAS*, 403, 996  
 Burstein D., Heiles C. 1982, *AJ*, 87, 1165  
 Fan X. 1999, *AJ*, 117, 2528  
 Fukugita M., Ichikawa T., Gunn J.E., Doi M., Shimasaku K., Schneider D.P. 1996, *AJ*, 111, 1748  
 Girardi L., Rubele S., Kerber L. 2009, *MNRAS*, 394, L74  
 Girardi L., Rubele S., Kerber L. 2010, *Proc. IAU Symp. Star Clusters - Basic Galactic Building Blocks throughout Time and Space*, Eds. R. de Grijs, J. Lepine, Cambridge University Press, Volume 266, 320  
 Glatt K., Grebel E.K., Koch A. 2010, *A&A* 517, 50  
 Goudfrooij P., Puzia T.H., Kozhurina-Platais V., Chandar R. 2009, *AJ*, 137, 4988  
 Goudfrooij P., Puzia T.H., Kozhurina-Platais V., Chandar R. 2011, *ApJ*, 737, 3  
 Haschke R., Grebel E.K., Duffau S. 2012, *AJ*, 144, 106  
 Keller S.C., Mackey A.D., Da Costa G.S. 2011, *ApJ*, 731, 22  
 Keller S.C., Mackey A.D., Da Costa G.S. 2012, *ApJ*, 761, L5  
 King I. 1962, *AJ*, 67, 471  
 Li Z., Mao C., Chen L., Zhang Q. 2012, *ApJ*, 761, L22  
 Mackey A.D., Broby Nielsen P. 2007, *MNRAS*, 379, 151  
 Mackey A.D., Broby Nielsen P., Ferguson M.N., Richardson J.C. 2008, *ApJL*, 681, L17  
 Marigo P., Girardi L., Bressan A., Groenewegen M.A.T., Silva L., Granato G.L. 2008, *A&A*, 482, 883  
 Milone A.P., Bedin L.R., Piotto G., Anderson J. 2009, *A&A*, 497, 755  
 Piatti A.E. 2011, *MNRAS*, 418, L40  
 Piatti A.E., Geisler D. 2012, *AJ*, 144, (in press, arXiv1208.3899)  
 Santiago B., 2009, in van Loon J. Th., Oliveira J. M., eds, *Proc. IAU Symp. 256, The Magellanic System: Stars, Gas, and Galaxies*, Cambridge Univ. Press, Cambridge, p. 69  
 Schlegel D.J., Finkbeiner D.P., Davis M. 1998, *ApJ*, 500, 525  
 Stetson P.B., Davis L.E., Crabtree D.R. 1990, in Jacoby G.H., ed., *ASP Conf. Ser. Vol 8, CCDs in Astronomy*, Astron. Soc. Pac., San Francisco, p. 289  
 Yang W., Meng X., Bil Sh., Tian Z., Li T., Liu K. 2011, *ApJL*, 731, L37

**Table 1.** CCD SDSS *gr* data of stars in the field of SL 529.

ID	$x$ (pixel)	$y$ (pixel)	$g$ (mag)	$\sigma(g)$ (mag)	$g-r$ (mag)	$\sigma(g-r)$ (mag)	$n$
...	...	...	...	...	...	...	...
19	787.031	1523.905	18.004	0.003	0.772	0.004	2
20	1198.930	767.067	18.007	0.007	-0.324	0.009	2
21	1651.733	1353.525	17.968	0.003	0.866	0.004	2
...	...	...	...	...	...	...	...